Infrared study of (H,Be)-, (D,Be)-, and (Li,Be)-acceptor complexes in silicon

R. E. Peale, K. Muro,* and A. J. Sievers
Laboratory of Atomic and Solid State Physics and Materials Science Center, Cornell University, Ithaca, New York 14853-2501

(Received 14 August 1989; revised manuscript received 16 November 1989)

The temperature and stress dependences of the $p_{1/2}$-series $2p'$ line for the acceptors (Li,Be), (D,Be), and (H,Be) in silicon have been measured. The results demonstrate that (Li,Be) is a fixed $\langle 111 \rangle$-oriented defect with a ground state split by local distortion and that (D,Be) and (H,Be) undergo either tunneling or hindered rotor motion. A far-infrared study of the ground-state splitting of (Li,Be) also reveals an unexpected 4-cm^{-1} line that, based on temperature-dependent infrared spectra, we have attributed to the neutral double-acceptor Be. Our results for (Li,Be) provide a standard to which the unusual features in the temperature and stress dependences of (D,Be) and (H,Be) can be compared. For both (D,Be) and (H,Be) we find a blue-shifted replica of the $2p'$ line and a ground-state manifold consisting of at least three well-resolved energy levels. This multiplet is explained by a tunneling model which we extend to give quantitative formulas for the stress dependence. Comparison of the model with our stress data provides additional evidence that (D,Be) and (H,Be) either tunnel or rotate between equivalent equilibrium orientations and that these orientations are along $\langle 111 \rangle$ directions, contrary to the results of recent numerical simulations.

I. INTRODUCTION

The discovery of the hydrogen passivation[1] of electronic defects in semiconductors has led to the discovery of many H-related complexes whose unusual properties are currently under investigation. Among these interesting centers are several donor and acceptor complexes in both silicon and germanium whose infrared (ir) spectra have been explained by models in which the defect tunnels among several equivalent configurations at low temperature.

One example is the triple acceptor Cu in Ge, which forms complexes with one, two, or three H atoms, with each H reducing the Cu's valence by 1. A study[2] of copper dihydrogen in Ge shows that this single acceptor has a complicated ground-state manifold and full tetrahedral symmetry. When heavier isotopes of H are substituted, the resulting defects have lower symmetry and only a single ground-state component. These observations are qualitatively explained by a model in which the H atoms rotate or tunnel around Cu with interaction between this nuclear motion and the acceptor's electronic states, but a quantitative theoretical model is lacking for this center.

A detailed model for the tunneling of H or Li around heavier substitutional impurities has been developed for the donors[3,4] (H,O) and (Li,O) and the acceptors[5] (H,C) and (H,Si) in Ge in order to explain their stress-dependent infrared spectra. However, recently it has been shown that the data are better explained by models in which these defects have fixed orientation and ground states split by local distortion.[6,7]

The same tunneling model[5] has also been used to explain the far-infrared (FIR) spectra and the temperature dependence of the ir spectra of the acceptors (H,Be) and (D,Be) in silicon.[8] At 1.7 K these acceptors have, in addition to the usual "$p_{3/2}$ series" of ir absorption lines, a weak *blue*-shifted replica of each line. For this to be possible, there must exist two levels of different energy for every excited energy level of an ordinary acceptor, so that the blue-shifted replica of each line corresponds to a transition from the common ground state to the upper level of each pair. As the sample temperature is raised, additional *red*-shifted replicas of the 1.7-K lines appear, showing that the ground-state consists of a manifold of at least three and probably four distinct energy levels. FIR measurements show three lines at 1.2 K and confirm the correctness of the assignment. The tunneling model[5] accounts for all these transitions, but it also predicts that as many as five distinct energy levels exist in the ground-state manifold. Unless some of these levels accidentally coincide, a complete spectrum has not been verified for (H,Be) and (D,Be) in silicon. The failure to observe all the levels predicted by theory leaves open the question of the uniqueness of the tunneling assignment and motivates further study.

In this paper we investigate the "$p_{1/2}$ series" of the acceptors (Li,Be), (D,Be), and (H,Be) in silicon under uniaxial compression. We also present the $p_{1/2}$-series temperature dependence for (D,Be) and (Li,Be) and the FIR spectrum for (Li,Be). The purpose of including (Li,Be), a low-symmetry defect with fixed orientation,[8] is both to establish its spectroscopic properties more firmly and to make our comparison with (D,Be) and (H,Be) systems more compelling. The FIR studies produced an additional spectral feature which we have been able to identify with the double-acceptor Be. High-resolution temperature-dependent ir spectra for Be in Si have been included to support this assignment. The temperature-dependent spectra for (D,Be) present a simpler, clearer picture than has been previously given[8] of temperature-induced changes, but no evidence for more than three en-

ergy levels in the ground-state manifold is found. The transition energies of (H,Be) and (D,Be) in Si as a function of stress adequately agree with the theoretical expectations and permit us to extract small values for a strain-coupling coefficient which indicates some splitting will remain unresolved. Our stress results in combination with the temperature dependence support the identification of (D,Be) and (H,Be) as tunneling systems, although the level spacings are more consistent with nearly free rotor motion. In spite of the lack of a complete spectrum, our results for (H,Be) and (D,Be) provide evidence that at liquid-helium temperature these defects tunnel or rotate among their equilibrium configurations along ⟨111⟩ directions, contrary to the results of recent numerical simulations.[9]

This paper is organized as follows. Section II A gives an overview of the well-known energy levels for single acceptors in silicon so that different groups of lines in the ir spectra presented here can be discussed using standard terminology, without ambiguity. The pertinent aspects of the tunneling model are presented next in Sec. II B. In this way the unusual features in the spectra of the acceptors (H,Be) and (D,Be) can be related directly to the known level symmetries and degeneracies predicted by a definite model. The effects of uniaxial stress are discussed in Sec. II C for both static and tunneling centers, and quantitative formulas for the splitting of nuclear tunneling states are given and plotted. The methods for sample preparation, data collection, and application of uniaxial stress are discussed in Sec. III. Section IV A presents temperature-dependent spectra for the two known centers caused by diffusion of Be into silicon. Section IV B gives the temperature- and stress-dependent ir spectra and an FIR spectrum of (Li,Be). Section IV C gives the temperature-dependent spectra for (D,Be) and stress-dependent spectra for both (D,Be) and (H,Be). Discussion and conclusions are contained in Sec. V.

II. CALCULATED STRESS SPLITTINGS

A. Acceptor Spectrum

The usual[10] $p_{3/2}$ and $p_{1/2}$ series of acceptor levels are given by the Hamiltonian

$$H_a = H_{el} - e^2/\epsilon r \ , \tag{1}$$

where H_{el} gives the energies of an unbound hole in the $p_{3/2}$ or split-off $p_{1/2}$ valence-band maximum, e is the electron charge, ϵ is the Si dielectric constant, and $\mathbf{r}$ is the hole coordinate. Figure 1 shows a schematic energy-level diagram for ordinary acceptors. Transitions from the $j=\frac{3}{2}$ ground state to excited states of both series are allowed, and two absorption series are observed[11] separated by the 345.5 cm^{-1} valence-band spin-orbit splitting[10] λ. Transitions from the $j=\frac{3}{2}$ ground state to the $j=\frac{1}{2}$ ground state are forbidden since these states have the same parity. The strongest line of the $p_{1/2}$ series is labeled[11] $2p'$ and is a Γ_8 to Γ_6 transition, where the Γ_i are irreducible representations of the tetrahedral (T_d) point group. We confine the present study to this line because of its relatively simple behavior under stress. The $3p'$ transition, though much weaker than the $2p'$ transition, does appear in our spectra, so we have indicated it in Fig. 1.

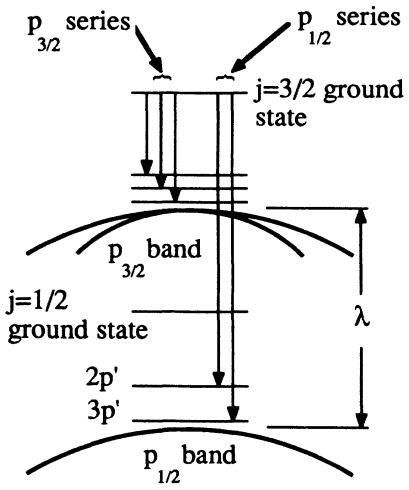

FIG. 1. Schematic energy-level diagram for a single acceptor. Energy levels derived from the $p_{3/2}$ and $p_{1/2}$ valence-band maxima and the corresponding $p_{3/2}$ and $p_{1/2}$ series transitions are indicated. The spin-orbit splitting is λ. The $2p'$ transition is the strongest in the $p_{1/2}$ series.

B. Tunneling model

The Hamiltonian for acceptors with nuclear-tunneling motion is[5]

$$H = H_a + H_n + V(\mathbf{r},\mathbf{R}) \ , \tag{2}$$

where H_n is the energy of nuclear motion and $V(\mathbf{r},\mathbf{R})$ is the energy of coupling between hole and nuclear motion. The nuclear coordinate is $\mathbf{R}$.

Four functions of $\mathbf{R}$ corresponding to the equivalent ⟨111⟩ defect orientations form a basis[5] for H_n. If the defect tunnels between these orientations, then the defect symmetry is effectively tetrahedral. The combinations of nuclear wave functions which diagonalize H_n must therefore give irreducible representations of T_d. The eigenvalues[5,7] of H_n are (E_n-3t), a Γ_1 singlet, and (E_n+t), a Γ_5 triplet. E_n is the matrix element of H_n diagonal with respect to nuclear orientation, and $-t$ is the matrix element of H_n between wave functions for different nuclear orientations. The product of nuclear and hole wave functions gives the total wave function, which belongs to $\Gamma_1\otimes\Gamma_i$ or $\Gamma_5\otimes\Gamma_i$, where Γ_i classifies the hole factor.

The term $V(\mathbf{r},\mathbf{R})$ is expected to be negligible for excited states because these have small amplitude at the nucleus. For a given excited-state level E_a, the total energy takes two values, (E_a+E_n-3t) and (E_a+E_n+t), corresponding to Γ_1 and Γ_5 nuclear tunneling states, respectively. The interaction term $V(\mathbf{r},\mathbf{R})$ may significantly mix the states belonging to lowest-lying $\Gamma_1\otimes\Gamma_8$ and $\Gamma_5\otimes\Gamma_8$ energy levels, partially lifting the twelvefold degeneracy of the $\Gamma_5\otimes\Gamma_8$ level and leading to a complicated

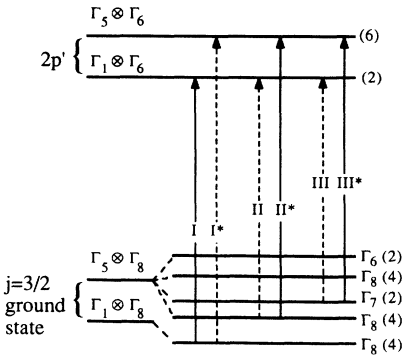

FIG. 2. Energy levels involved in $2p'$ transition when tunneling is present. When the interaction $V(\mathbf{r},\mathbf{R})$ between nuclear and electronic motion is zero, shown on the left, each ordinary-acceptor level is replaced by a pair of levels. The states belonging to the upper level of each pair are products of a Γ_5-type nuclear wave function and a Γ_6 or Γ_8-type hole wave function. The states belonging to the lower level of each pair are products of a Γ_1 type nuclear wave function and a Γ_6- or Γ_8 hole wave function. When $V(\mathbf{r},\mathbf{R})$ is nonzero, shown on the right, the pair of tunneling-acceptor levels corresponding to the $j=\frac{3}{2}$ ordinary-acceptor ground level splits into a manifold of up to five levels whose symmetries are given on the right. The degeneracies of each level, including spin degeneracy, is given in parentheses. Some ir transitions are indicated. Those represented by solid lines are allowed and those represented by dashed lines are weakly allowed.

ground-state manifold. In any case, the lowest level of the tunneling-acceptor system is the fourfold degenerate $\Gamma_1\otimes\Gamma_8=\Gamma_8$ level, and this has the same symmetry and degeneracy as an ordinary acceptor ground state.

Figure 2 shows the tunneling-acceptor energy-level diagram for a $j=3/2$ ground state to $2p'$ transition. The left-hand side of Fig. 2 shows the energy levels and their symmetries when the interaction $V(\mathbf{r},\mathbf{R})$ between nuclear and electronic motion is zero. The right-hand side shows the levels and their symmetry when $V(\mathbf{r},\mathbf{R})$ is nonzero where up to five energy levels now exist in the ground-state manifold. The degeneracy remaining in each level, including spin degeneracy, is given in parentheses. At very low temperature, only transitions from the lowest level of the ground-state manifold should be seen, labeled I and I*. As the temperature is raised, up to eight additional absorption lines may appear. Four of these are labeled in Fig. 2 as II, II*, III, and III*. Transitions between states of different nuclear symmetry are forbidden, since the electric-dipole operator does not act on functions of $\mathbf{R}$. Thus, transition I* is forbidden unless the states in its initial level are given a sufficient admixture of Γ_5-type nuclear states by the interaction $V(\mathbf{r},\mathbf{R})$. Similarly, transition II and III will not be observed unless $V(\mathbf{r},\mathbf{R})$ is large enough. In any case, we should observe transition I* weaker than transition I, II weaker than II*, and III weaker than III*. In Fig. 2, the strong transitions are depicted by solid arrows and the weak ones by dashed arrows.

C. Uniaxial stress

For an acceptor without internal structure, the $2p'$ line of the $p_{1/2}$ series splits[12] for any stress direction because the fourfold degenerate Γ_8 ground level splits in two. The Γ_6 excited level is a Kramers doublet and does not split. The relative strength of the two components of the split $2p'$ transition changes with increasing stress due to thermal depopulation of the split ground level's upper component. For example, for Si(B), the $2p'$ splitting is isotropic.[12]

For an acceptor with internal structure of lower symmetry than T_d, the Γ_8 ground level in general is split by local distortion into a pair of Kramers doublets. Each absorption line has a red-shifted replica which gains strength as the temperature is raised. External stress can alter the magnitude of the ground-level splitting already present from local distortion, but it cannot cause further splitting of the levels involved. Nevertheless, the $2p'$ absorption line appears to split since there are several equivalent, but not identical, defect orientations with different stress behavior. As an example, consider a $\langle 111\rangle$-oriented defect. Under $\langle 111\rangle$ stress those defects oriented in the direction parallel to the stress will experience a different energy shift than the defects whose orientations are in the other three directions, causing the $2p'$ line to split with a temperature-independent 3:1 absorption-strength ratio. Tensional (compressional) local distortion causes the stronger component to be higher (lower) in frequency when external compression is applied.[6] Under $\langle 110\rangle$ stress, the $2p'$ line splits with a 1:1 strength ratio. Stress along $\langle 001\rangle$ causes no splitting since the four orientations are still equivalent. Quantitative formulas for the stress dependence of this type of acceptor may be found in Ref. 6.

If the internal structure of an acceptor defect tunnels between its equivalent configurations, there are two kinds of transitions from the lowest component of the ground-state manifold, and these behave differently under stress. Excited energy levels having Γ_1-type nuclear symmetry split in the same way as ordinary acceptor excited levels. The splitting of excited energy levels having Γ_5-type nuclear symmetry is more complicated since, in addition to electronic degeneracy, such levels also have threefold nuclear degeneracy. To illustrate this splitting behavior, we present quantitative formulas[7] for the stress-dependent energies of nuclear tunneling states. The detailed comparison of our data with the expected lifting of level degeneracy and stress-tuned interactions between the various nuclear tunneling states will provide another test of the tunneling model.[5]

Under arbitrarily-directed uniaxial stress, all nuclear tunneling states share the linear hydrostatic shift $(\Theta_d+\Theta_u/3)(2s_{12}+s_{11})T$. We do not include this energy in the equations that follow. Θ_u and Θ_d are strain-coupling coefficients, s_{ij} are the silicon elastic-compliance coefficients, and T is the stress magnitude.

Stress along $\langle 111\rangle$ reduces the symmetry to C_{3v}. A Γ_5 level splits into a singlet Λ_1 and a doublet Λ_3, and a Γ_1 level becomes Λ_1, where Γ_i and Λ_i are irreducible representations of the point groups T_d and C_{3v}, respectively.

The energies of the new levels are

$$E(\Gamma_1(\Lambda_1))=\tfrac{1}{9}\Theta_u s_{44}T-t-2[t^2+\tfrac{1}{9}\Theta_u s_{44}tT+(\tfrac{1}{9}\Theta_u s_{44}T)^2]^{1/2}\ , \quad (3)$$

$$E(\Gamma_5(\Lambda_1))=\tfrac{1}{9}\Theta_u s_{44}T-t+2[t^2+\tfrac{1}{9}\Theta_u s_{44}tT+(\tfrac{1}{9}\Theta_u s_{44}T)^2]^{1/2}\ , \quad (4)$$

$$E(\Gamma_5(\Lambda_3))=-\tfrac{1}{9}\Theta_u s_{44}T+t\ . \quad (5)$$

Stress along ⟨110⟩ splits a Γ_5 level into Λ_1, Λ_2, and Λ_3, and Γ_1 becomes Λ_1, where the Λ_i are now irreducible representations of C_{2v}. The energies of the new levels are given by

$$E(\Gamma_1(\Lambda_1))=-t-[4t^2+(\tfrac{1}{12}\Theta_u s_{44}T)^2]^{1/2}\ , \quad (6)$$

$$E(\Gamma_5(\Lambda_1))=-t+[4t^2+(\tfrac{1}{12}\Theta_u s_{44}T)^2]^{1/2}\ , \quad (7)$$

$$E(\Gamma_5(\Lambda_2))=t+\tfrac{1}{12}\Theta_u s_{44}T\ , \quad (8)$$

$$E(\Gamma_4(\Lambda_3))=t-\tfrac{1}{12}\Theta_u s_{44}T\ . \quad (9)$$

Under ⟨001⟩ stress, Γ_5 becomes $\Lambda_4\oplus\Lambda_5$, and Γ_1 becomes Λ_1, where the Λ_i refer to irreducible representations of D_{2d}. The levels do not split since all ⟨111⟩ orientations are equivalent for this stress direction.

Equations (3)–(9) are plotted in Fig. 3 as a function of $(\frac{1}{9})\Theta_u s_{44}T$. The two types of nuclear symmetry are indicated on the left, and their zero-stress separation is $4t$. In Fig. 3, we use the value of $t=4.05$ cm^{-1} found previously[8] for (D,Be). Only ⟨111⟩- and ⟨110⟩-stress dependences are shown, plotted with solid and dashed lines, respectively, since ⟨001⟩ stress has no effect. Both the magnitude and the curvature of the splitting is greater for ⟨111⟩ than for ⟨110⟩ stress.

III. EXPERIMENTAL DETAILS

The starting material for all samples is float-zone silicon of resistivity 1600–2000 Ω cm. For (H,Be) and (D,Be) samples, about 1 μm of Be is evaporated onto both faces of a 5×10×25-mm^3 sample, which is then sealed in a quartz ampoule together with 500 Torr He and 200 Torr H_2 or D_2 gas, heated at 1300 °C for 20 min and quenched in air. Contact between the quartz and the sample is prevented by a thin layer of carbon created by heating in a flame a quartz tube whose inside is wet with acetone.

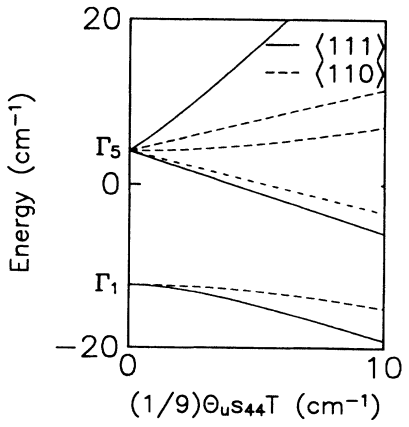

FIG. 3. Calculated splitting of the nuclear tunneling states for ⟨111⟩ and ⟨110⟩ stress. We neglect shifts common to all components. The nuclear symmetry is given on the left.

For (Li,Be) samples, Be-coated starting material sealed with 700 Torr He in an unsooted quartz ampoule is heated at 1300 °C for 0.5 h and slowly quenched by turning off the furnace. Clean Li is then rubbed on the sample which is subsequently heated at 380 °C for 0.5 h in a sealed ampoule filled with 700 Torr He. Excess Li is removed by scraping the sample with a razor blade and washing with water. A final 2-h anneal at 600 °C in an evacuated ampoule is found to be necessary to remove free-carrier absorption due to excess Li in the sample. Finally, all samples are mechanically polished.

During the measurements, the sample is immersed in 1.7-K pumped liquid helium in a Janis varitemp cryostat. Elevated sample temperatures were obtained by heating either the sample mount or the capillary through which liquid helium (LHe) enters the cryostat's sample chamber. The temperature was monitored with a calibrated 1-kΩ Allen-Bradley resistor. The cryostat's tailstock is introduced through an o-ring muff-coupler to the evacuated sample compartment of a Bruker Fourier-transform infrared (FTIR) interferometer. Optical access to the cryostat sample chamber is provided by NaCl and ZnSe windows. The spectra presented here were recorded at either 1.0 or 0.5 cm^{-1} resolution.

Uniaxial stress is applied by means of calibrated weights, levers, and a piston. The stress is buffered by cardboard, plastic tape, or indium at the ends of the sample. Of these, cardboard seemed to give the least inhomogeneous broadening to the spectral features. The piston is prevented from imparting a twisting force by being composed of two lengths coupled by a ball bearing. The magnitude of the stress is determined by mechanical considerations.

To obtain FIR spectra, a lamellar grating interferometer and a ^{3}He-cooled Ge bolometer detector were used. The spectrum presented below was collected at 0.25 cm^{-1} resolution. The same sample was used for these measurements as was used for the (Li,Be) ⟨111⟩-stress experiment, but here the FIR radiation is passed through the long axes of the sample to insure deep absorption lines.

IV. RESULTS

A. Be in silicon

The absorption bands of Be in silicon are well known,[13–15] but since the early spectra were taken with low-resolution grating spectrometers at sample temperatures no lower than 8 K, spectra taken at higher resolution with FTIR at sample temperatures as low as 1.7 K are presented here to provide improved accuracy. As will be shown, several novel features are revealed. Be in

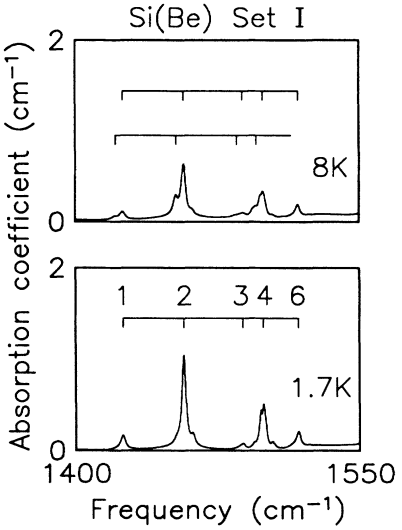

FIG. 4. Temperature dependent set I $p_{3/2}$-series absorption spectra of the neutral double-acceptor Be in Si. The absorption coefficient is plotted vs the frequency in wave numbers. The bottom portion gives the spectrum at a sample temperature of 1.7 K. The main lines are indicated and numbered in the standard way. The top spectrum was taken at a sample, temperature of 8 K, where, in addition to the original series, a replica red shifted by 4 cm^{-1} is evident, as indicated.

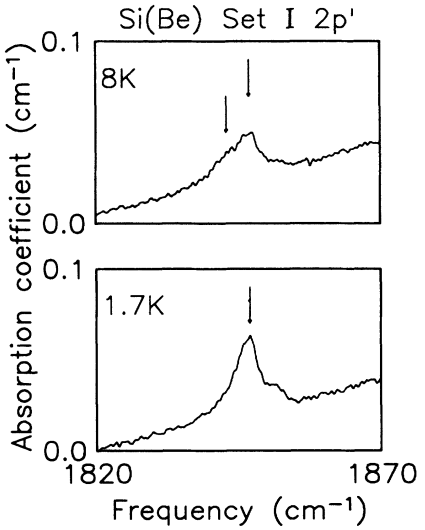

FIG. 5. Temperature dependence of the $2p'$ line of Si(Be)'s set I $p_{3/2}$ series. Absorption coefficient is plotted vs frequency in wave numbers. In the 1.7-K spectrum (bottom) the $2p'$ line is indicated by an arrow. In the 8-K spectrum, a low-frequency shoulder has appeared centered 4 cm^{-1} from the $2p'$ line, and these two features are indicated by arrows.

silicon introduces two acceptor levels whose ir absorption lines are labeled[13–15] set I and set II. Figure 4 gives the spectra of the $p_{3/2}$ series of set I at 1.7 and 8 K. At 1.7 K an acceptor absorption series is observed, and the strongest lines are labeled by conventional numbering.[10] As the temperature is raised, a red-shifted replica appears and gains intensity with increasing temperature, as shown in the 8-K spectrum. The separation of the replica from the main series is 4.0 cm^{-1}. If the defect responsible for the set I absorption series is the substitutional neutral double-acceptor Be^0, then these data may be explained by a 4.0-cm^{-1} splitting of the sixfold degenerate two-hole ground state by the hole-hole interaction.[16,17] As the temperature is raised, the upper level becomes thermally populated, and transitions from it to the excited states appear. A ground-state splitting of 4 cm^{-1} has also been deduced from the deconvoluted line shapes of the set I $p_{3/2}$ series by Heyman *et al.*[18]

Heyman *et al.*[18] have also reported the observation of lines belonging to the $p_{1/2}$ series of set I. Figure 5 gives the temperature dependence of the $2p'$ line of set I's $p_{1/2}$ series. The strong peak in the 1.7-K spectrum has a high-frequency shoulder, but no such shoulder appears in the spectrum of the single-acceptor boron in silicon.[10] We shall not speculate as to its origin since our purpose for including Fig. 5 is solely to illustrate changes which occur in Be's set I $2p'$ line as the sample temperature is raised. The strong peak in Fig. 5 is 1 order of magnitude weaker than the lines of the $p_{3/2}$ series shown in Fig. 4, so its temperature dependence is expected to be correspondingly more difficult to interpret. Nonetheless, the 8-K spectrum shows a definite low-frequency shoulder absent in the 1.7-K spectrum, and this shoulder is centered at about 4 cm^{-1} from the main peak. The main peak and its 8-K shoulder are indicated by arrows in Fig. 5. This result is consistent with the model for acceptor transitions shown in Fig. 1, in which both $p_{1/2}$ and $p_{3/2}$ series share the same initial state.

Interestingly, the set II $p_{3/2}$ series for Be in Si shows no evidence of a split ground state. Figure 6 presents the

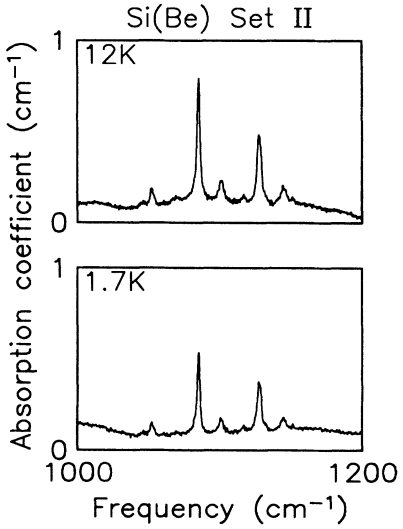

FIG. 6. Temperature dependence of the Si(Be) set II $p_{3/2}$ series. Absorption coefficient is plotted vs frequency in wave numbers for sample temperatures of 1.7 (bottom) and 12 (top) K. No new features appear as the temperature is raised, indicating that the ground state of this acceptor consists of a single component.

absorption spectra at 1.7 and 12 K. Both spectra look the same, and no red-shifted replica appears at any temperature up to 50 K, at which point the lines have all but disappeared due to thermal ionization. Quenching and annealing studies[14] have shown that set II is due to a more complex Be configuration than set I. Set II can be identified with either a single acceptor or a double acceptor. A complex defect may cause a local distortion which lifts the fourfold single-acceptor ground-state degeneracy, and the sixfold double-acceptor ground-state degeneracy may be lifted completely by both local distortion and hole-hole interaction.[16,17] Since we observe no splitting at all, the question of whether this center binds one or two holes remains open. However, the simplest microscopic model[14] is that of two Be atoms occupying nearest-neighbor substitutional sites. This defect may be viewed as a divacancy into which two Be atoms are placed. The valence electrons of the Be atoms together satisfy four of the divacancy's six dangling bonds. The two remaining bonds are completed by capturing two electrons from the valence band, and the center as a whole remains neutral by binding two holes. Such a defect would be a double acceptor, and so it has been argued[14] that set II may be identified as the spectrum of a double acceptor.

B. (Li,Be) in silicon

Lithium forms a complex with each of the Be-related centers in silicon.[14] If both of the original centers are double acceptors, a likely scenario is that Li resides in one of the nearest-neighbor tetrahedral interstitial sites[19] and fills a silicon bond with its valence electron.[14] In this way the Be centers are partially passivated, and the resulting defects are single acceptors. Two sets of absorption lines due to these (Li,Be) acceptor complexes appear[8,14,15] in the ir spectra, and these are labeled[14] set I and set II as was done for the Be centers. We ignore set II in this paper. The absorptions of set I for (Li,Be) in Si are shown in the bottom part of Fig. 7. Here silicon bulk absorption is divided out by plotting the ratio of 1.7 and 100-K spectra, and the ordinate scale is 0 to 2. The $p_{3/2}$ series appears at low frequency. At higher frequency, the $2p'$ line,[10] the strongest of the $p_{1/2}$ series, is indicated by an arrow. The sharp line at 1136 cm^{-1} is an interstitial-oxygen vibrational mode.[20]

The temperature dependence of the (Li,Be) $2p'$ line is shown in Fig. 8. A single line is visible at 1.7 K, but as the temperature is raised a red-shifted replica appears and gains in relative strength, as shown in the 30-K spectrum. The peak positions of the main line and its replica are separated by 11.1 cm^{-1}. Similar results have already been reported for the lines of the $p_{3/2}$ series, where a separation of[14] 9.7 and[8] 11.3 cm^{-1} has been found. All three values are the same within experimental uncertainty, but we consider the value 11.3 cm^{-1} to be closest to the true value since it was obtained from the many strong sharp lines of the $p_{3/2}$ series using the highest spectral resolution.

Figure 9 gives the FIR absorption spectrum from 2 to 25 cm^{-1} of a silicon sample into which both Be and Li have been diffused. The instrumental resolution is 0.25 cm^{-1}. The line at 11.5 cm^{-1} we attribute to the transition between the components of the (Li,Be)'s split ground state. The agreement with the 11.3-cm^{-1} splitting implied by the temperature dependence of the ir spectra is within experimental uncertainty.

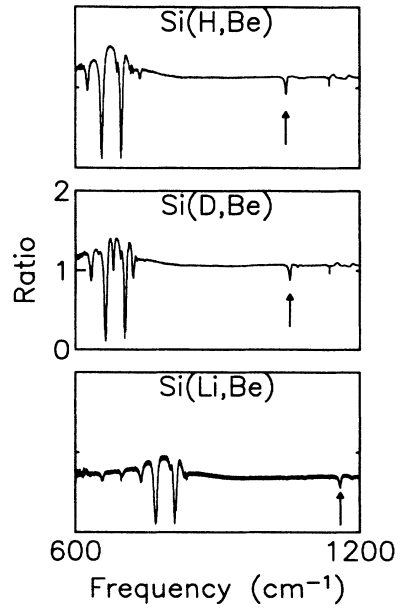

FIG. 7. Transmission spectra for the acceptors (H,Be),(D,Be), and (Li,Be) in silicon. The ratio of spectra made at sample temperatures of 1.7 and 100 K is plotted vs frequency in wave numbers in order to eliminate Si bulk absorption. The ordinate scale for each spectrum is the same. In each spectrum, the $p_{3/2}$ series is at low frequency and the $2p'$ line of the $p_{1/2}$ series is indicated by an arrow.

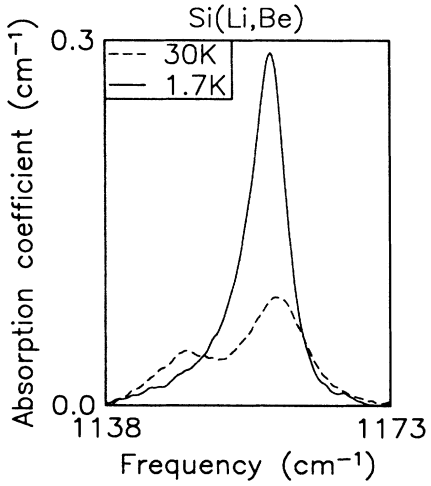

FIG. 8. Temperature dependence of the (Li,Be) $2p'$ line. Absorption coefficient vs frequency in wave numbers is plotted. The 1.7-K spectrum (solid line) shows only the $2p'$ line. The 30-K spectrum (dashed line) reveals a single $2p'$-line replica red shifted by 11.1 cm^{-1}.

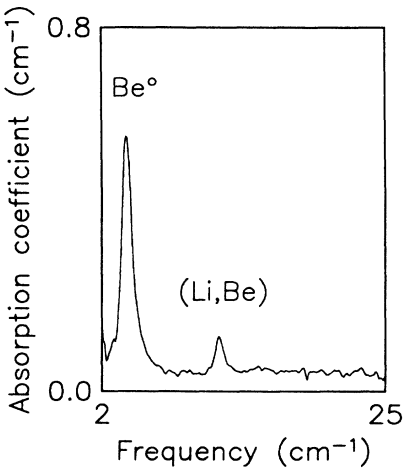

FIG. 9. Far-infrared spectrum of silicon doped with both Be and Li. Absorption coefficient vs frequency in wave numbers is plotted. The line at 11.5 cm^{-1} corresponds to the transition between the two components of (Li,Be)'s split ground level. The line at 4 cm^{-1} is the transition between components of the split ground level of the neutral double-acceptor Be^0 in Si. The experimental resolution is 0.25 cm^{-1}, and the sample temperature is 1.2 K.

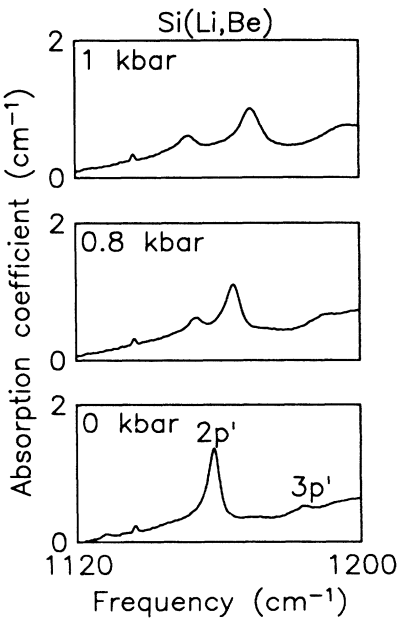

FIG. 10. Spectra of the $p_{1/2}$ series of (Li,Be) in silicon under ⟨111⟩ compression. Absorption coefficient vs frequency in wave numbers is plotted. At zero stress (bottom) both $2p'$ and $3p'$ transitions are observed as indicated. At a stress of 1 kbar (top), the $2p'$ line has clearly split into two components with a strength ratio of 1:3. The sample temperature is 1.7 K.

The strong line at 4.0 cm^{-1} in Fig. 9 is identified with the transition between the ground-state components of the neutral double-acceptor Be^0. The same ground-state splitting was found in Figs. 4 and 5 for the temperature dependence of Be's set I absorption lines. Since these absorption lines are still present in the ir spectra after Li diffusion, enough Be centers remain to account for a strong FIR line. The 4-cm^{-1} line is also found in the FIR spectra of Si(Be), Si(H,Be), and Si(D,Be), but not in samples which do not contain Be.

Figure 10 gives spectra of (Li,Be) in Si for three values of ⟨111⟩ uniaxial compression. The same sample was used here as in the FIR experiment. The $2p'$ and $3p'$ transitions are labeled, and the magnitude of the stress in units of kbar is indicated above each spectrum. The $2p'$ line clearly splits, and the components have a line-strength ratio of roughly 3:1 with the stronger component higher in frequency. The line strength ratio appears to be independent of the magnitude of the splitting, so there is no evidence for thermal redistribution of level populations.

Figure 11 shows plots of the center frequencies of the observed components of the stress-split (Li,Be) $2p'$ line for compression along ⟨111⟩, ⟨110⟩, and ⟨001⟩. The $2p'$ line splits into two for ⟨111⟩ stress with a strength ratio of approximately 3:1 where the stronger component is higher in frequency. Both components exhibit an upwards curvature similar to that observed in the stress-dependent $2p'$-line transition energies of boron in silicon.[10] Stress along ⟨110⟩ splits the $2p'$ line into two components of roughly equal strength. The magnitude of this splitting is smaller than for ⟨111⟩ stress. For ⟨001⟩ stress, no splitting or broadening of the $2p'$ line is observed, and we find a maximum upwards shift of only 1

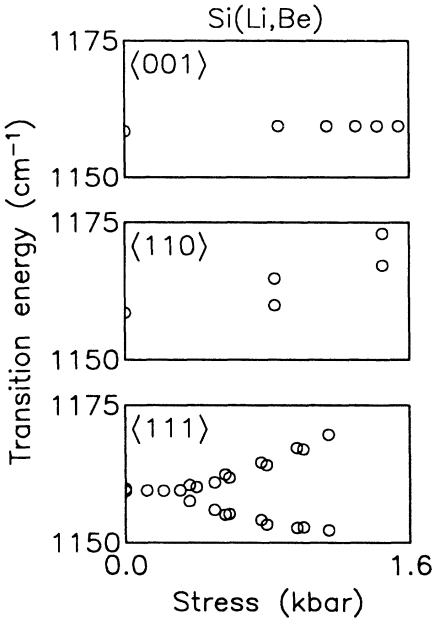

FIG. 11. Dependence of the (Li,Be) $2p'$ line for stress along the three principal axes. The center frequencies of all observed components of the $2p'$ line are plotted vs the magnitude of the applied uniaxial compression. Data for stress along ⟨100⟩, ⟨110⟩, and ⟨111⟩ axes are given at top, middle, and bottom, respectively. All these data were collected at a sample temperature of 1.7 K.

cm^{-1}, which is the same as the instrumental resolution. All these data imply[6] that (Li,Be) in Si has a static ⟨111⟩ orientation whose configurational degeneracy can be lifted by externally applied stress, and that the defect gives rise to a C_{3v} distortion which splits the acceptor Γ_8 ground state by 11.3 cm^{-1}.

C. (D,Be) and (H,Be) in silicon

Hydrogen[8,15] and deuterium[8] also form complexes with both Be centers in silicon, and two sets of single-acceptor absorption lines appear in analogy with (Li,Be) in Si and Be in Si. The top and middle spectra of Fig. 7 show the lines of set I for (H,Be) and (D,Be) respectively. We ignore set II in this paper. In Fig. 7 silicon bulk absorption is divided out by plotting the ratio of 1.7- and 100-K spectra, and the ordinate scale is the same for each spectrum. The $p_{3/2}$ series appear at low frequency. The lines for (H,Be) are lower in frequency[8] than the lines for (D,Be) by 7.8 cm^{-1}, and this isotope shift is just visible at this scale. More lines than are usually present in a $p_{3/2}$ series appear in (D,Be)'s spectrum. Corresponding lines in the $p_{3/2}$ series of (H,Be) also exist, but they are weaker and partly hidden by coincidence with the main lines. Closer inspection[8] reveals that the additional lines form an exact blue-shifted replica of the $p_{3/2}$ series. The separation of the replica from the main series is 16.2 cm^{-1} for (D,Be) and 38.8 cm^{-1} for (H,Be).

At higher frequencies in Fig. 7, the $2p'$ line of the $p_{1/2}$ series is indicated in each spectrum by an arrow. These lines also display weak blue-shifted replicas, invisible at this scale, whose separations are the same as were found for the $p_{3/2}$ series. These features are discussed in detail in the following paragraphs. The sharp line at 1136 cm^{-1} is an interstitial-oxygen vibrational mode.[20]

Figure 12 gives the absorption spectrum of the $2p'$ line of (D,Be) in Si at temperatures of 1.7, 8, and 15 K. In the 1.7-K spectrum, a weak *blue*-shifted replica (labeled I*) of the $2p'$ line (labeled I) appears 16.2 cm^{-1} above the (D,Be) $2p'$ line, just as was found for the lines of the $p_{3/2}$ series.[8] The $3p'$ line appears as a small bump above I* in frequency, so that the I* line cannot be attributed to any of the known $p_{1/2}$-series acceptor lines. As the sample temperature is raised first one and then another *red*-shifted replica of lines I and I* appear. These replicas are labeled II, II*, III, and III* in Fig. 12. Line III may exist as a broadening of the low-energy shoulder of lines I and II, but it does not clearly emerge at any temperature. Its expected position relative to line I, as indicated in Fig. 12, is found from the measured separation of lines I* and III*. Its label in Fig. 12 has been placed in parentheses to indicate this uncertainty. At higher temperatures, the line widths become so large that it is no longer possible to resolve any additional replicas which might be present. Clearly, the acceptor (D,Be) has a manifold of at least three low-lying energy levels. Furthermore, the existence of the low-temperature *blue*-shifted replica I* of line I shows that the final level of an ordinary-acceptor $2p'$ transition is replaced for (D,Be) by a pair of energy levels. This energy-level scheme cannot be caused by a local distortion since this gives a maximum of two low-lying energy levels. Moreover, local perturbations do not affect the nonlocal excited states, and the twofold spin degeneracy of an ordinary-acceptor $2p'$ level can only be lifted by a magnetic field. This defect system evidently has additional degrees of freedom.

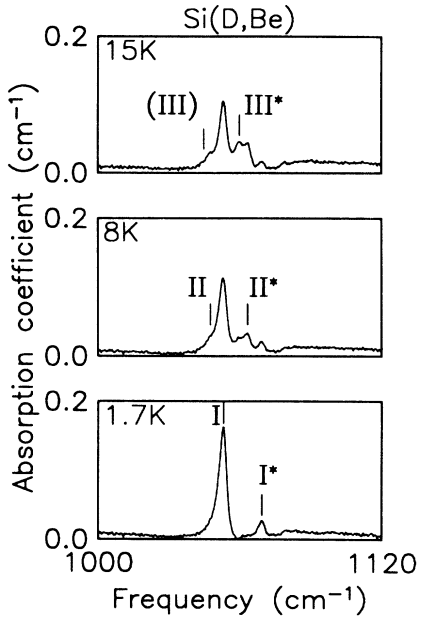

FIG. 12. Temperature dependence of $2p'$ line of (D,Be) in Si. Absorption coefficient vs frequency in wave numbers is plotted. the 1.7-K spectrum (bottom) shows that the $2p'$ line (I) has a *blue*-shifted replica (I*). At 8 K (middle), a *red*-shifted replica (II and II*) of lines I and I* is evident. At 12 K (top), at least one line (III*) of yet another red-shifted replica can be discerned. Above 15 K the lines become too broad to identify any additional replicas which might appear.

The fact that the $2p'$ line of the (D,Be) acceptor has a weak *blue*-shifted replica at 1.7 K suggests that the temperature dependence could be explained by the detailed tunneling model (Fig. 2) of Haller *et al.*[5,8] Then the transitions shown in Fig. 2 correspond to the absorption lines with the same labels in Fig. 12. Notice that in Fig. 12, line I* is weaker than line I, line II is weaker than line II*, and line III is weaker than line III*. This is exactly what is predicted from Fig. 2 where solid arrows show strong transitions and dashed arrows show weak transitions. If Fig. 2 gives the correct ordering of the levels in the low-lying manifold, then transition III originates from a level of Γ_7 symmetry. Since each term in the Hamiltonian Eq. (2) must be invariant under the operations of the tetrahedral group, i.e., must transform as Γ_1, the interaction $V(\mathbf{r},\mathbf{R})$ cannot mix the lowest Γ_8 level with the Γ_7 level. In other words, the initial level of transition III has only Γ_5-type nuclear symmetry, whereas the final level has only Γ_1-type nuclear symmetry. Thus, the transition III in Fig. 2 should be strictly forbidden, and this is in agreement with the failure in Fig. 12 to observe a definite line at the position expected for line III. Likewise, in the original work of Muro and Sievers[8] no lines III were observed in the temperature dependence of

(D,Be)'s $p_{3/2}$ series.

According to the tunneling model, the ground-state manifold contains as many as five distinct energy levels. Unless some of these levels accidentally coincide, Fig. 12 does not give the complete spectrum, so there is value in studying this system in the presence of some other perturbation such as stress. Figure 13 shows the absorption spectra of (D,Be) in Si under ⟨111⟩ uniaxial compression. The magnitude of the stress in kbar and the identification of absorption lines I and I* are given above each spectrum. Both lines undergo a large upwards shift in frequency and broaden, but neither is observed to split. If Fig. 2 gives (D,Be)'s energy levels, then the initial level of transitions I and I* has the same Γ_8 symmetry and fourfold degeneracy as an ordinary acceptor and should split under stress. Two transitions will be present when the splitting is on the order of kT so that both components of the stress-split initial level are populated. The sample temperature during the measurements shown in Fig. 13 was 1.7 K, which corresponds to only 1.2 cm^{-1} in energy, and the zero-stress line width is already 5 cm^{-1}. The upper component of the split ground level will be unpopulated at 1.7 K for any splitting large enough to be resolved as two lines. Thus, it is reasonable that the expected stress splitting of the initial level of the transitions I and I* does not appear in Fig. 13.

In order to test this idea, we have looked at the stress spectra at elevated temperature. Figure 14 gives the spectra of (D,Be) in Si at 6 K for three values of stress.

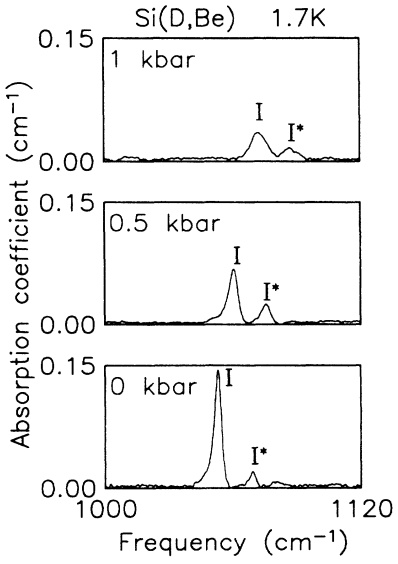

FIG. 13. Stress-dependent spectra of the $2p'$ line for (D,Be) in Si at 1.7 K. Absorption coefficient vs frequency in wave numbers is plotted. In each part of this figure the I and I* lines (Fig. 12) are indicated. As the ⟨111⟩ stress is increased from zero (bottom) to 0.5 (middle), to 1 kbar (top), both lines shift to higher frequency and broaden. Line I* increases in strength relative to line I. At 1 kbar the shape of the line I* indicates that it may consist of two components. The peaks of lines I and I* also converge slightly. The sample temperature is too low for the expected stress splitting of the initial level of transitions I and I* to be resolved.

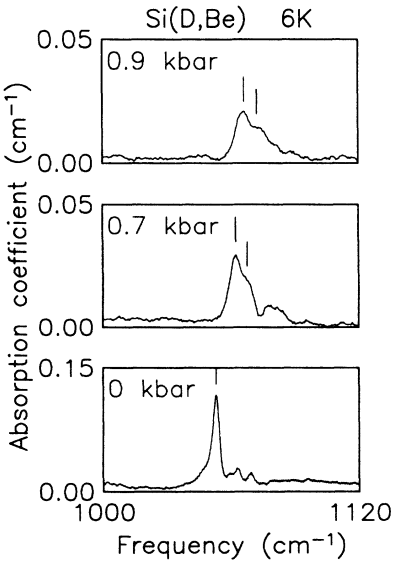

FIG. 14. Stress-dependent spectra of the $2p'$ line for (D,Be) in Si at 6 K. Stress is applied along a ⟨111⟩ axis. Absorption coefficient is plotted vs frequency in wave numbers for stress values of 0 (bottom), 0.7 (middle), and 0.9 (top) kbar. Here the temperature is high enough that both components of the stress-split initial level are populated up to the largest stress values. This ground-level splitting is observed as a splitting of line I as indicated by the vertical lines above the spectra.

The top two spectra have been partially smoothed to reduce the size of interference fringes, and the ordinate scale is smaller than in the bottom spectrum in order to bring out the details of the stress-broadened lines. Sloping baselines in all three spectra have been corrected. At zero stress (bottom) line I is indicated by a vertical bar above it. Also, line I* is observed, replicas II* and III* appear between I and I*, and replica II has broadened the low-frequency tail of line I. At a stress value of 0.7 kbar (middle), the unusual shape of line I suggests that it is composed of two components, as indicated by the vertical lines above the spectrum. At a stress value of 0.9 kbar (top), this suggestion is even stronger, and the two components, indicated by vertical lines, appear to have moved farther apart. Though the two components are never fully resolved, their separation appears to be about 5 or 6 cm^{-1}, which is considerably less than the 24-cm^{-1} splitting found at 0.9 kbar for the $2p'$ line of the shallow-acceptor boron in silicon.[10] This difference suggests strong mixing between (D,Be)'s low-lying levels. A temperature of 6 K corresponds to 4 cm^{-1} in energy, so both components of a ground-level split by about 5 cm^{-1} should be populated, and two transitions should be observed. These observations are consistent with the energy-level diagram Fig. 2 in which the lowest level has the same Γ_8 symmetry and fourfold degeneracy as an ordinary acceptor.

According to Fig. 2, the final level of the I transition has only spin degeneracy and should not split under stress. However, the final level of the I* transition has, in addition to the twofold spin degeneracy, a threefold nu-

clear degeneracy, since three nuclear tunneling states of Γ_5-type symmetry belong to this energy level. Figure 3 shows that a Γ_5-type nuclear tunneling level should split in two for ⟨111⟩ stress. Therefore, a 1.7-K spectrum of Si(D,Be) under sufficiently large ⟨111⟩ stress should reveal a splitting of line I*, but not of line I. In Fig. 13 the unusual shape of line I* at 1.1 kbars indicates that there may be two components present, but the splitting is not resolved. The I and I* peaks converge slightly with stress, suggesting that I* is dominated by its degenerate Λ_3 component at high stress. From the measured peak separation and Fig. 3, we judge that our measurements extend only to a $\frac{1}{9}\Theta_u s_{44} T$ value of about 2 cm^{-1} at $T=1$ kbar, giving a value of $\Theta_u s_{44}$ of approximately 18 cm^{-1}/kbar.

The possibility that the two components of a stress-split I* line might be polarized differently was investigated by placing a wire grid polarizer in the beam of the FTIR in front of the cryostat. Spectra were collected for the beam polarized either parallel or perpendicular to the direction of the applied compression. No conclusive evidence for a difference in the spectra for the two polarization directions was discovered because the I* line at high stress is very broad and its peak is not very much higher than the baseline noise level, as seen in Fig. 13.

Figure 13 also shows that the strength of line I* relative to line I increases with stress. A calculation of the fraction of the Γ_1-type nuclear tunneling state from the final level of transition I mixed by stress into the nuclear tunneling states in the final level of transition I* shows that stress mixing of the states in the final levels is insufficient to account for the oscillator-strength increase. The main source must be mixing by stress of the nuclear tunneling states belonging to the low-lying energy levels in the ground-state manifold. This calculation is complicated by the mixing already present from the interaction $V(\mathbf{r},\mathbf{R})$, and it has not been attempted.

The situation is similar for (H,Be) in Si. At 1.7 K the $2p'$ line has a weak blue-shifted replica separated by 38.8 cm^{-1}, as found previously[8] for the $p_{3/2}$ series. The main line (I) and its replica (I*) shift upwards in energy and converge slightly, but do not split when uniaxial stress is applied to a sample at 1.7 K. Since the separation $4t$ of levels with different nuclear symmetry is larger for (H,Be) than for (D,Be), mixing within the ground-state manifold by $V(\mathbf{r},\mathbf{R})$ is smaller. Line I* of (H,Be) is weaker relative to line I than for (D,Be), and the stress splitting of line I* should be both smaller and more difficult to resolve.

The ⟨111⟩-stress dependence of the $2p'$ lines I and I* of (D,Be) and of (H,Be) in Si at 1.7 K is summarized in Fig. 15. The (D,Be) data are given by circles and the (H,Be) data by triangles. Zero-stress transitions are labeled on the left border by their final-level nuclear symmetry, Γ_1 or Γ_5. Stress-split components are labeled on the right border.

The curves in Fig. 15 were found as follows. Since lines I and I* converge slightly with stress, line I* must be dominated by its degenerate Λ_3 component, according to Fig. 3. To simplify the analysis we assume that the measured I* peak position gives the frequency of its Λ_3 component. From these points, for each value of stress, we subtract the center frequency of line I, which eliminates both the stress dependence of their initial level and the hydrostatic shift common to the excited states. We fit the difference of Eq. (5) and Eq. (3) to these data, using[8] $t=4.05$ cm^{-1} for (D,Be) and $t=9.7$ cm^{-1} for (H,Be). This fit yields values for $\Theta_u s_{44}$ of 16.5±0.5 (D,Be) and 19±2 (H,Be) cm^{-1}/kbar, in agreement with our crude estimate above. Using[21] $s_{44}=1.246\times10^{-3}$ $kbar^{-1}$ gives values for Θ_u of $(1.32\pm0.04)\times10^4$ cm^{-1} (D,Be) and $(1.5\pm0.2)\times10^4$ cm^{-1} (H,Be), which are the same within experimental uncertainty. We find the combined excited-state hydrostatic and ground-state shift by fitting the I* data to a second-order polynomial and subtracting points calculated from Eq. (5). By adding the result to Eqs. (3)–(5), we obtain the curves plotted in Fig. 15. The curve for I* must, of course, match the data closely because of the procedure used to find it. The dashed line predicts the position for the Λ_1 component of line I* if the assumption that our data primarily show the Λ_3 component (solid line) of line I* is correct. The separation of these two curves is less than the experimental high-stress I* line width (Fig. 13) consistent with our inability to resolve the splitting. The curve for line I agrees well with the data.

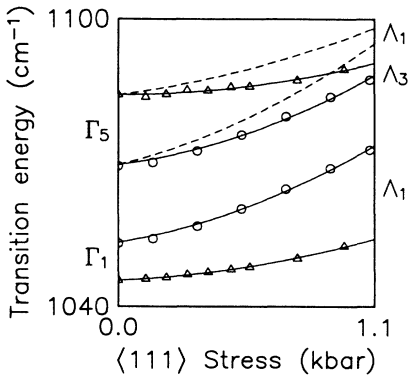

FIG. 15. Center frequencies of the $2p'$ lines I and I* as a function of ⟨111⟩ stress for (D,Be) and (H,Be) in silicon. The (H,Be) and (D,Be) data are represented by open triangles and open circles, respectively. The type of the nuclear part for final-state wave functions is shown on the left for T_d symmetry and on the right for C_{3v} symmetry. The solid lines represent a fit of the peak frequencies to theory, and the dashed lines predict the frequency position of the unresolved Λ_1 component of the I* line. These data were collected at a sample temperature of 1.7 K so that initial-level splitting does not interfere with the analysis.

Since the excited-state stress dependence is nearly linear at low stress (Fig. 3), the large curvature observed in the transition energies (Fig. 15) belongs primarily to the lowest level of the ground-state manifold. By analogy with Fig. 3, both the magnitude and curvature of the ground-state shift should decrease in changing from ⟨111⟩ to ⟨110⟩ and from ⟨110⟩ to ⟨001⟩ stress, if the defect equilibrium orientation is along ⟨111⟩. Figure 16

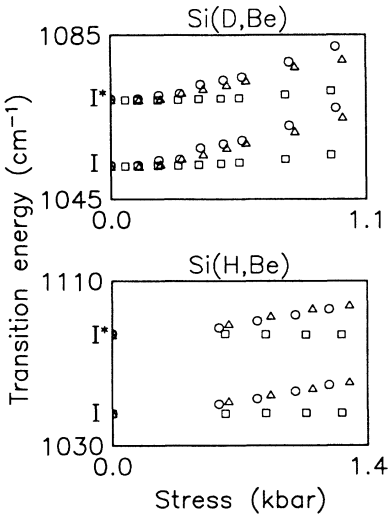

FIG. 16. Center frequencies of the $2p'$ lines I and I* of (H,Be) and (D,Be) in silicon as a function of stress along the three principal axes. The open circles, open triangles, and open squares represent data for ⟨111⟩, ⟨110⟩, and ⟨001⟩ stress, respectively. The smallest energy shifts are seen for ⟨001⟩ stress. For (D,Be) (top), the largest shifts are seen for ⟨111⟩ stress, which implies a ⟨111⟩ equilibrium orientation. For (H,Be) (bottom) the shifts for ⟨111⟩ and ⟨110⟩ stress are comparable. These data were collected at a sample temperature of 1.7 K.

is a plot of the transition energies of the $2p'$ lines I and I* as a function of stress along the principal crystallographic axes. The upper and lower parts of Fig. 16 give the data for (D,Be) and (H,Be), respectively. Data for ⟨111⟩, ⟨110⟩, and ⟨001⟩ stress are represented by open circles, open triangles, and open squares, respectively. As expected, there is almost no shift for ⟨001⟩ stress for either defect. The shift with ⟨110⟩ stress clearly lies between that for ⟨001⟩ and ⟨111⟩ stress for (D,Be). For (H,Be), ⟨111⟩ and ⟨110⟩ stress give the same shift within experimental uncertainty. Since the Γ_5 line is quite weak and broad for (H,Be), it is difficult to measure its center frequency precisely. Thus, it is not at variance with the available data to say that the equilibrium orientation of *both* (H,Be) and (D,Be) are along a ⟨111⟩ direction.

V. DISCUSSION AND CONCLUSIONS

The temperature dependence and stress behavior of the $2p'$ line for the acceptors (Li,Be), (D,Be), and (H,Be) in silicon has been measured, and the results for (D,Be) and (H,Be) are fundamentally different from those for (Li,Be). For (Li,Be) the stress splitting of the $2p'$ line is consistent with the model of a fixed ⟨111⟩-oriented defect whose ground state is split by local distortion. The temperature dependence of the $2p'$ line and FIR spectroscopy gives direct evidence of this splitting.

The stress splitting of the $2p'$ transition's initial state observed for (D,Be) in silicon at 6 K shows that this level has the degeneracy expected for the ground level of an acceptor in tetrahedral symmetry. For this to be true, reorientational motion must occur since (D,Be) itself has symmetry lower than T_d. A weak blue-shifted replica of the $2p'$ line of (D,Be) and (H,Be) in Si at 1.7 K requires that there be a pair of distinct energy levels corresponding to the final level of an ordinary acceptor's $2p'$ transition. Temperature dependence of the $2p'$ line for (D,Be) reveals the existence of a low-lying manifold of at least three distinct energy levels. All these features are adequately explained by the detailed tunneling model of Haller *et al.*[4,7] Following Ham,[7] we have extended this model to give quantitative formulas for the expected stress dependence. A fit of our (D,Be) and (H,Be) data to this model yields values for the strain-coupling coefficent θ_u, which imply that the predicted, but unobserved, splitting of the 1.7-K $2p'$-line replica is masked by the experimental line widths. We estimate that a stress of at least 2 kbars will be necessary to resolve this splitting, and this is beyond the present capability of our apparatus.

Data at higher values of stress than that presented here might help decide if the model of Ham[7] given in Eqs. (3)–(9) and Fig. 3 for the splitting of nuclear tunneling states correctly gives the relative motion of the various stress-split components. According to this model the $\Gamma_5(\Lambda_3)$ and $\Gamma_1(\Lambda_1)$ components should asymptotically converge to a separation of $3t$ from a zero-stress separation of $4t$. A different model developed to explain the stress dependence of the donors (H,O) and (Li,O) in Ge by Joós *et al.*[3] assumes that $\Gamma_5(\Lambda_1)$ and $\Gamma_1(\Lambda_1)$ do not mix and predicts that $\Gamma_5(\Lambda_3)$ and $\Gamma_1(\Lambda_1)$ components cross for sufficiently large ⟨111⟩ stress, but this behavior has been argued to be unphysical.[7] Our experiments do not extend far enough in stress to distinguish between the two cases, so the question of which model correctly applies to (D,Be) and (H,Be) in silicon remains open, in principle.

In constructing a basis of nuclear wave functions, the tunneling model[5] assumes that the equilibrium positions of the H or D lie along ⟨111⟩ directions. However, recent pseudopotential-density-functional calculations[9] suggest that H should rest midway between any two of Be's nearest neighbors, which would give the defect six equivalent ⟨001⟩ orientations. If this were true, Eqs. (3)–(9) would not give the correct stress dependence. In particular, ⟨100⟩ rather than ⟨111⟩ stress should cause the largest shift in the transition energies. This prediction is not in agreement with our observations plotted in Fig. 16; hence, we conclude that the equilibrium orientations of (H,Be) and (D,Be) are truly along ⟨111⟩ contrary to the results of Ref. 9.

There is one fundamental problem which remains with the tunneling model. It was found that the excited levels of the acceptors (D,Be) and (H,Be) exist in pairs separated by the tunneling energy with a value of 16.2 cm^{-1} (D,Be) and 38.8 cm^{-1} (H,Be), respectively. However, for a freely rotating $(H\text{-}Be)^-$ molecule, the energy separations between $J=0$ and 1 rotational states are 21.1 cm^{-1} (H,Be) and 11.6 cm^{-1} (D,Be) assuming that the bond length of the defect in Si is the same as in the free neutral molecule[22] ($r=1.333$ Å). These values for the energy separations of rotational levels are *less* than the observed separations of the tunneling levels, although free rotation should be the *upper* limit as tunneling becomes more rapid.

Since the isotope spacing is nearly the same as that of a free rotor and since the two lowest energy states of a free rotor are Γ_1 and Γ_5 there is some value in exploring the possibility that free rotor behavior is responsible for the pairs of excited-state levels which have been observed. (Presumably, higher angular-momentum states would be above the band edge.) Larger values for the lowest rotational energies can be obtained if we assume that the H sits halfway between the Be and its nearest Si neighbor and if Be is assumed to be fixed in a substitutional position. Then the H mass instead of the reduced mass appears in the moment of inertia, and the Be-H separation is only 1.18 Å. The rotational energies are then 24.2 cm^{-1} (H,Be) and 12.1 cm^{-1} (D,Be), still smaller than the observed level separations. If we ask what Be-H or Be-D separations will give rotational energies that are equal to the observed level spacings, we find that Be and H are separated by 0.9 Å and that Be and D are separated by 1 Å. One possibility consistent with the observed isotope effect would be that free rotor behavior occurs for (H,Be) separated by an internuclear distance of 0.9 Å and that (D,Be) acts somewhat hindered giving a smaller energy spacing.

In conclusion, the expected, but unobserved, levels in the ground-state manifold, unresolved stress splitting in the excited states, and the unusually large separation of tunneling levels for the acceptors (D,Be) and (H,Be) in silicon indicate that there is still much to be learned about the dynamics of these centers. Nonetheless, the data presented here provide strong evidence that these defects either tunnel or rotate. As such, they now represent the only acceptor (or donor) complexes in semiconductors quantitatively explained by an explicit dynamical nuclear model without a competing static-defect interpretation.

ACKNOWLEDGMENTS

The authors would like to thank G. D. Watkins for useful comments and F. S. Ham for a critical reading of the manuscript. This work was supported by the National Science Foundation under Grant No. DMR-87-14600 and by the U. S. Army Research Office (ARO) under Grant No. DAAL03-86-K-0103.

---

*Permanent address: High Performance Research Laboratories, Mitsui Petrochemical, Ltd., Nagaura, Sodegaura-machi, Kimitsu-gun, Chiba 299-02, Japan.

[1]S. J. Pearton, J. W. Corbett, and T. S. Shi, Appl. Phys. A **43**, 153 (1987).

[2]J. M. Kahn, L. M. Falicov, and E. E. Haller, Phys. Rev. Lett. **57**, 2077 (1986).

[3]B. Joós, E. E. Haller, and L. M. Falicov, Phys. Rev. B **22**, 832 (1980).

[4]E. E. Haller and L. M. Falicov, Phys. Rev. Lett. **41**, 1192 (1978).

[5]E. E. Haller, B. Joós, and L. M. Falicov, Phys. Rev. B **21**, 4729 (1980).

[6]J. M. Kahn, R. E. McMurray, Jr., E. E. Haller, and L. M. Falicov, Phys. Rev. B **36**, 8001 (1987).

[7]F. S. Ham, Phys. Rev. B **38**, 5474 (1988).

[8]K. Muro and A. J. Sievers, Phys. Rev. Lett. **57**, 897 (1986).

[9]P. J. H. Denteneer, C. G. Van de Walle, and S. T. Pantelides, Phys. Rev. Lett. **62**, 1884 (1989).

[10]A. K. Ramdas and S. Rodriguez, Rep. Prog. Phys. **44**, 1297 (1981).

[11]S. Zwerdling, K. J. Button, B. Lax, and L. M. Roth, Phys. Rev. Lett. **4**, 173 (1960).

[12]H. R. Chandrasekhar, P. Fisher, A. K. Ramdas, and S. Rodriguez, Phys. Rev. B **8**, 3836 (1973).

[13]J. B. Robertson and R. K. Franks, Solid State Commun. **6**, 825 (1968).

[14]R. K. Crouch, J. B. Robertson, and T. E. Gilmer, Phys. Rev. B **5**, 3111 (1972).

[15]R. K. Crouch, J. B. Robertson, H. T. Morgan, T. E. Gilmer, and R. K. Frank, J. Phys. Chem. Solids **35**, 833 (1974).

[16]E. Kartheuser and Sergio Rodriguez, Phys. Rev. B **8**, 1556 (1973).

[17]D. Labrie, I. J. Booth, M. L. W. Thewalt, and E. E. Haller, Phys. Rev. B **38**, 5504 (1988).

[18]J. Heyman, L. M. Falicov, and E. E. Haller, Bull. Am. Phys. Soc. **34**, 834 (1989).

[19]R. L. Aggarwal, P. Fisher, V. Mourzine, and A. K. Ramdas, Phys. Rev. **138**, 686 (1967).

[20]D. R. Bosomworth, W. Hayes, A. R. L. Spray, and G. D. Watkins, Proc. R. Soc. London, Ser. A **317**, 133 (1970).

[21]J. J. Hall, Phys. Rev. **161**, 756 (1967).

[22]G. Herzberg, *Spectra of Diatomic Molecules* (Van Nostrand, New York, 1950), p. 508.